

# Synthesis, Characterization, and Photocatalytic Activity of Titania and Niobia Mesoporous Molecular Sieves

Victor F. Stone, Jr. and Robert J. Davis\*

Department of Chemical Engineering, University of Virginia,  
Charlottesville, Virginia 22903-2441

Received January 27, 1998. Revised Manuscript Received March 20, 1998

Mesoporous titania and niobia molecular sieves were prepared by a ligand-assisted templating method. For comparison, titania samples were also prepared by simple hydrolysis and condensation of Ti alkoxide in the absence of templating agents. All materials were thoroughly characterized by UV–vis reflectance spectroscopy, N<sub>2</sub> adsorption, and X-ray diffraction. The UV absorption thresholds, and thus the optical band gaps, of as-synthesized mesoporous titania and niobia were similar to those of bulk phase, crystalline reference materials. Adsorption of N<sub>2</sub> showed that extremely high surface area materials were synthesized by the templating method as long as thermal treatments were moderate. Higher temperature caused loss in surface area and partial crystallization of the sample. Elemental analysis revealed that neither high-temperature calcination nor solvent extraction removed the phosphorus component of the template used in the synthesis of mesoporous titania. However, solvent extraction of the template was effective for the mesoporous niobia sample. The transition metal oxides were tested as photocatalysts in the liquid-phase oxidative dehydrogenation of 2-propanol to acetone. The observed quantum yield of the reaction was 0.45 over Degussa P25, a standard titania catalyst. However, mesoporous titania converted 2-propanol with a very low quantum yield of 0.0026. Amorphous titania synthesized by alkoxide hydrolysis also exhibited a very low photocatalytic activity for the reaction. The quantum yield increased as the amorphous titania was crystallized to greater extents. A very low quantum yield was also found for the mesoporous niobia sample compared to a crystalline standard. Apparently, the surface reactivities of the poorly crystallized samples were suppressed by defects that act as electron–hole traps.

## Introduction

Semiconducting transition metal oxides participate in a variety of photocatalytic reactions including oxidative degradation of organics,<sup>1–5</sup> reduction of metal ions,<sup>6</sup> evolution of dihydrogen from water,<sup>7–12</sup> and fixation of carbon dioxide.<sup>13–17</sup> Due to its low cost, ease of handling, and high resistance to photoinduced corrosion,

titanium dioxide is one of the most studied semiconductors for these photocatalytic reactions. Titania is a wide band gap semiconductor that absorbs photons in the near-UV region, thus limiting its use in solar-based applications. Nevertheless, photocatalytic systems utilizing titania with artificial UV sources have been applied to the remediation of contaminated water sources.

The effectiveness of titania as a photocatalyst depends on its crystal phase, particle size, and crystallinity. Among the common crystalline forms of titania, anatase is generally recognized to be the most active phase. With regard to particle size, smaller particles are usually better photocatalysts due to their high surface area-to-volume ratios. However, the band gap is a strong function of titania particle size for diameters less than 10 nm, which can be attributed to the well-known quantum size effect.<sup>18–20</sup> Particles in this size range have extremely high surface areas, but the blue shift in usable photon energies with decreasing size limits

\* To whom correspondence should be addressed.

(1) Ollis, D. F.; Al-Ekabi, H., Eds. *Photocatalytic Purification and Treatment of Water and Air*; Elsevier: Amsterdam, 1993.

(2) Mills, A.; Davies, R. *J. Photochem. Photobiol. A: Chem.* **1995**, *85*, 173.

(3) Al-Sayyed, G.; D'Oliveira, J. C.; Pichat, P. *J. Photochem. Photobiol. A: Chem.* **1991**, *58*, 99.

(4) Davis, R. J.; Gainer, J.; O'Neal, G.; Wu, I.-W. *Water Environ. Res.* **1994**, *66*, 50.

(5) Vindogopal, K. *Environ. Sci. Technol.* **1995**, *29*, 841.

(6) Tanaka, K.; Harada, K.; Murata, S. *Sol. Energy* **1986**, *36*, 159.

(7) Karakitsou, K.; Verykios, X. E. *J. Catal.* **1995**, *152*, 360.

(8) Munuera, G.; Soria, J.; Conesa, J. C.; Sanz, J.; Gonzalez-Elipe, A. R.; Navio, A.; Lopez-Molina, E. J.; Munoz, A.; Fernandez, A.; Espinos, J. P. In *Catalysis on the Energy Scene*; Kaliaguine, S., Mahay, A., Eds.; Elsevier: Amsterdam, 1984; p 335.

(9) Bard, A. J.; Fox, M. A. *Acc. Chem. Res.* **1995**, *28*, 141.

(10) Sayama, K.; Tanaka, A.; Domen, K.; Maruya, K.; Onishi, T. *J. Catal.* **1990**, *124*, 541.

(11) Henderson, M. A. *Langmuir* **1996**, *12*, 5093.

(12) Tabata, S.; Nishida, H.; Masaki, Y.; Tabata, K. *Catal. Lett.* **1995**, *34*, 245.

(13) Saladin, F.; Forss, L.; Kamber, I. *J. Chem. Soc., Chem. Commun.* **1995**, 533.

(14) Yamagata, S.; Nishijo, M.; Murao, N.; Ohta, S.; Mizoguchi, I. *Zeolites* **1995**, *15*, 490.

(15) Malati, M. A. *Energy Convers. Manage.* **1996**, *37*, 1345.

(16) Anpo, M.; Yamashita, H.; Ichihashi, Y.; Ehara, S. *J. Electroanal. Chem.* **1995**, *396*, 21.

(17) Yamashita, H.; Kamada, N.; He, H.; Tanaka, K.-I.; Ehara, S.; Anpo, M. *Chem. Lett.* **1994**, 855.

(18) Brus, L. E. *J. Chem. Phys.* **1984**, *80*, 4403.

(19) Brus, L. *J. Phys. Chem.* **1986**, *90*, 2555.

(20) Wang, Y.; Suna, A.; Mahler, W.; Kasowski, R. *J. Chem. Phys.* **1987**, *87*, 7315.

their usefulness. Clearly, an optimum particle size balances the appropriate band gap with the high surface area needed for adsorption of molecules. The influence of degree of crystallinity on photocatalytic activity is much less understood.

Very recently, Ohtani et al. performed an elegant set of photocatalytic experiments on partially crystallized titania samples.<sup>21</sup> In that study, amorphous titania powders were calcined at various temperatures to accomplish fractional crystallization. Anatase was the only ordered phase of titania detected by X-ray diffraction. Since crystallization was accompanied by a very small change in overall surface area, the resulting set of titania samples was used to determine directly how the degree of crystallinity affects photocatalytic activity. Their results unambiguously showed that photocatalytic activity of amorphous titania was negligible compared to that of crystalline anatase particles of similar size. Low activity was attributed to the recombination of  $e^-$  and  $h^+$  at surface and bulk traps, which are presumably lattice defects. The authors also suggested that recombination reactions in the bulk traps were probably predominant in their amorphous samples; however, a quantitative analysis had not been performed.

Experiments with extremely high surface area titania samples are needed to clarify the role of surface traps in photocatalysis. Unfortunately, dense titania particles with extremely high surface areas also exhibit quantum size effects, which complicates the interpretation of reactivity experiments. Therefore, new forms of titania having high surface areas and similar band gaps need to be investigated.

High surface area titania and niobia mesoporous molecular sieves were recently synthesized by a ligand-assisted templating method.<sup>22,23</sup> In that procedure, organometallic precursors hydrolyze, condense, and self-assemble in the presence of surfactant molecules to form well-ordered mesoscopic solid structures. The method is similar to that developed by researchers at Mobil for the liquid crystal templating of MCM-41 mesoporous aluminosilicates,<sup>24,25</sup> but involves a strong interaction of the surfactant headgroup with the inorganic phase. Antonelli and Ying claim that removal of the surfactant molecules from the transition metal oxides results in very high surface area molecular sieves having unidimensional, hexagonally arranged mesopores. Even though their pore structures are well-ordered, these materials are considered amorphous, since no well-defined oxide crystal structures are detected by X-ray diffraction.

To the best of our knowledge, the photon absorption characteristics and photoactivities of these new materials have not been evaluated. This report describes the synthesis, characterization, and photocatalytic activity

of high surface area titania and niobia mesoporous molecular sieves.

## Experimental Methods

**Materials Synthesis.** The preparation of titania mesoporous molecular sieves was adapted from the procedure reported by Antonelli and Ying.<sup>22</sup> Due to its availability, the surfactant dodecyl phosphate was used in our work instead of tetradecyl phosphate used by Antonelli and Ying. Mono-dodecyl phosphate was purchased from Alfa-Aesar, while all other chemicals were obtained from Aldrich and used without modification.

Potassium hydroxide (0.49 g) was dissolved in deionized, distilled water (25 mL), and the pH was adjusted to 5.0 with HCl. The dodecyl phosphate (3.75 g) was then dissolved in this solution, mixed for at least 4–5 h, and aged quiescently for 6 h.

Titanium isopropoxide precursor (5.0 g) was mixed with acetylacetone (0.9 mL) in a separate flask and immediately added to the surfactant solution. The resulting slurry was placed into a Teflon-lined autoclave and heated to 353 K for at least 5 days without agitation. The product was isolated by vacuum filtration and washed three times with deionized, distilled water. After air-drying overnight at 393 K, the powder was examined by X-ray diffraction performed on a Scintag XDS 2000 diffractometer equipped with a  $Cu K\alpha$  radiation source.

We used two different procedures to remove the surfactant from the pores of the materials. The first method was calcination for 1 h in flowing dry air after heating with a ramp rate of 1 K  $min^{-1}$ . The second method was a liquid-phase extraction of the surfactant. This procedure was based on that of Antonelli and Ying as described in their paper on synthesis of mesoporous niobia.<sup>23</sup> An as-synthesized mesoporous material was added to a solution of nitric acid in ethanol (25 mL, approximately 1 M in ethanol), mixed, and then filtered. This was repeated before the material was washed with deionized, distilled water. Some samples were exposed to additional extraction solutions, as noted.

As a control, titania was also synthesized by hydrolysis and condensation of the titanium precursor in the absence of surfactant, denoted as *ns*-TiO<sub>2</sub>. Titanium isopropoxide was simply added dropwise to deionized distilled water. The resulting white powder was collected by vacuum filtration and dried in air at 393 K overnight.

Mesoporous niobia was also synthesized according to the methods of Antonelli and Ying.<sup>23</sup> In this case, the surfactant tetradecylamine was mixed with niobium ethoxide (5.0 g) without prior complexation. Ethanol (5 mL) and deionized, distilled water (15 mL) were quickly added, and the resulting slurry was transferred into a Teflon-lined autoclave. The autoclave was heated without agitation to 353, 373, and 453 K for 1, 1, and 7 days, respectively. The product was recovered by vacuum filtration; washed three times each with water, ethanol, and ether; and subsequently dried in air at 393 K overnight. The extraction method used for surfactant removal was similar to that described above, but diethyl ether was added to the washing solutions. The acid strength, however, remained the same.

Dinitrogen adsorption isotherms were recorded on a Coulter Omnisorb 100CX automated sorption apparatus.

A Varian Cary 3E system equipped with a Labsphere diffuse reflectance accessory was used to obtain the reflectance spectra of the materials over a range of 190–800 nm. Labsphere USRS-099-020 was employed as a reflectance standard. Direct band gaps of these materials were determined by plotting  $(\alpha h\nu)^2$  versus excitation energy (where  $\alpha$  is the absorption coefficient, determined from the Kubelka–Munk function) and extrapolating the linear part of the curve to  $(\alpha h\nu)^2 = 0$ .<sup>26–28</sup>

(21) Ohtani, B.; Ogawa, Y.; Nishimoto, S.-i. *J. Phys. Chem.* **1997**, *101*, 3746.

(22) Antonelli, D. M.; Ying, J. Y. *Angew. Chem., Int. Ed. Engl.* **1995**, *34*, 2014.

(23) Antonelli, D. M.; Ying, J. Y. *Angew. Chem., Int. Ed. Engl.* **1996**, *35*, 426.

(24) Beck, J. S.; Vartuli, J. C.; Roth, W. J.; Leonowicz, M. E.; Kresge, C. T.; Schmitt, K. D.; Chu, C. T.-W.; Olson, D. H.; Sheppard, E. W.; McCullen, S. B.; Higgins, J. B.; Schlenker, J. L. *J. Am. Chem. Soc.* **1992**, *114*, 10834.

(25) Kresge, C. T.; Leonowicz, M. E.; Roth, W. J.; Vartuli, J. C.; Beck, J. S. *Nature* **1992**, *359*, 710.

(26) Bube, R. H. *Electronic Properties of Crystalline Solids—An Introduction to Fundamentals*, Academic Press: New York, 1974.

(27) Davis, R. J. *Chem. Mater.* **1992**, *4*, 1410.

(28) Weber, R. S. *J. Catal.* **1995**, *151*, 470.

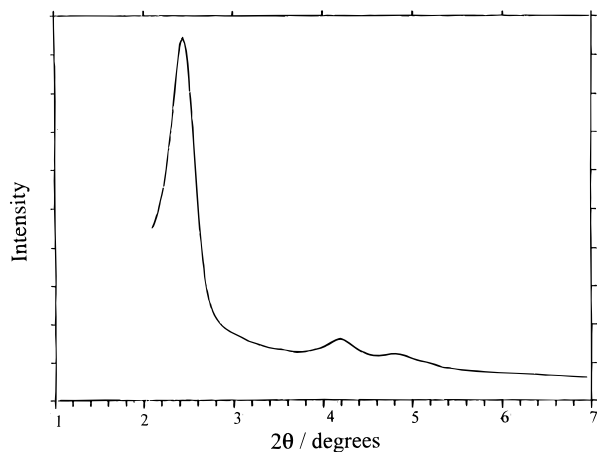


**Figure 1.** Low-angle X-ray diffraction pattern of as-synthesized mesoporous titania.

**Photocatalytic Reaction.** The reactor was a round-bottom, 50-mL Pyrex flask with a ground glass neck and a single port on the side of the vessel used for sample withdrawal. The top of the reactor was connected to a condenser to prevent losses of reactant and product. The reaction slurry was well-stirred by a magnetic stir bar and continuously sparged with dioxygen (Airco Gases) flowing at a rate of 2 mL min<sup>-1</sup>. The light source was an ILC Technology model R 150-9 150-W xenon arc lamp. The light first passed through a copper(II) sulfate solution to absorb long wavelengths. Optical filters were placed after the copper sulfate to select a peak transmitted wavelength of about 360 nm. Ferrioxalate actinometry was used to measure the number of photons entering the reactor, which was  $3.36 \times 10^{16}$  photons per second.<sup>29</sup> The apparent quantum yield reported here is based on the number of acetone molecules formed per incident photon.

The conditions used for the reaction were based on earlier studies in our laboratory.<sup>30</sup> Approximately equal volumes of 2-propanol (Aldrich) and deionized, distilled water were introduced into the reactor to give a total volume of about 50 mL. In a typical run, 0.4 g of catalyst was added to the system and the reactor was subsequently purged with flowing dioxygen for 30 min before irradiation. All runs were conducted at ambient pressure and temperature. Liquid samples were analyzed by gas chromatography (Hewlett-Packard 5850 Series II, equipped with an HP Econo-Cap capillary column connected to a flame ionization detector) after catalyst particles were removed by microfiltration.

## Results

The X-ray diffraction pattern of as-synthesized mesoporous titania is given in Figure 1. The large peak at low angle is typical for samples synthesized in the presence of surfactant. In addition, the small peaks at higher angles have been attributed to hexagonal ordering of mesopores in these solids.<sup>24,25</sup> However, Putnam et al. showed recently that lamellar phases can also exist in samples with similar X-ray patterns.<sup>31</sup> Figure 2 shows the typical dinitrogen adsorption/desorption isotherm for our material. Clearly, the onset of capillary condensation at moderate relative pressures and the negligible hysteresis loop at high relative pressures confirmed that the mesopores were fairly regular after

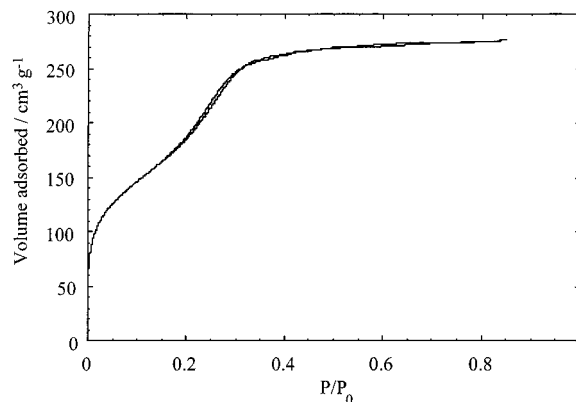


**Figure 2.** Dinitrogen adsorption/desorption isotherms of mesoporous titania calcined at 473 K.

**Table 1. Characterization and Reactivity Results for Titania Materials**

sample	surface area (m <sup>2</sup> g <sup>-1</sup> )	band gap (eV)	quantum yield <sup>a</sup>
meso-TiO <sub>2</sub> (473 K)	712	3.19	0.0026
meso-TiO <sub>2</sub> (973 K)	90	3.25	0.0089
meso-TiO <sub>2</sub> , extracted <sup>b</sup>	603	3.15	0.010
ns-TiO <sub>2</sub> , as-synthesized		3.24	0.0094
ns-TiO <sub>2</sub> (873 K), 1 h	39		0.022
ns-TiO <sub>2</sub> (873 K), 3 h	36	3.22	0.038
ns-TiO <sub>2</sub> (873 K), 12 h	28	3.26	0.27
anatase (Aldrich)	9	3.28	0.41
Degussa P25	50	3.22	0.45

<sup>a</sup> Quantum yield is defined as the molecules of acetone formed per incident photon. <sup>b</sup> Surfactant was extracted three times with 8% nitric acid in ethanol.

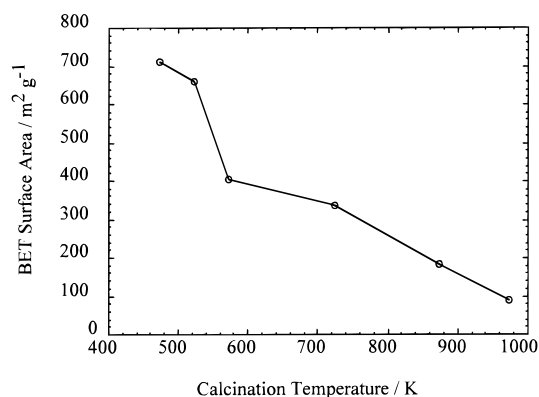


**Figure 3.** Effect of calcination temperature on surface area of mesoporous titania.

low-temperature calcination at 473 K. The major peak in the pore size distribution, calculated using the Horvath-Kawazoe method, occurs at about 24 Å, which is significantly smaller than the pore size reported by Antonelli and Ying (32 Å) for a similar material. However, the surfactant chain length used in the current work was 2 carbon units shorter than that used by Antonelli and Ying.

The BET surface area of the mesoporous titania after low-temperature calcination was extremely large, 712 m<sup>2</sup> g<sup>-1</sup>, and reproducible. The surface areas of other representative titania materials are summarized in Table 1. The calcined materials that were exposed to high temperatures showed substantial pore damage and loss in surface area, as depicted in Figure 3.

All of the mesoporous materials that were calcined turned from a yellow color (as-synthesized) to a dark

(29) Braun, A. M. *Photochemical Technology*; John Wiley & Sons: Chichester, 1991.

(30) Lee, J. D. *Influence of Carbonate Salts on the Photocatalytic Dehydrogenation of 2-Propanol*; M.S. Thesis, University of Virginia, 1993.

(31) Putnam, R. L.; Nakagawa, N.; McGrath, K. M.; Yao, N.; Aksay, I. A.; Gruner, S. M.; Navrotsky, A. *Chem. Mater.* **1997**, *9*, 2690.

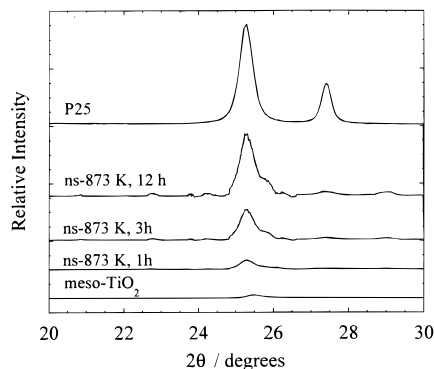


**Figure 4.** X-ray diffraction patterns showing the presence of anatase and rutile in various titania samples. Meso-TiO<sub>2</sub> was calcined for 1 h at 873 K.

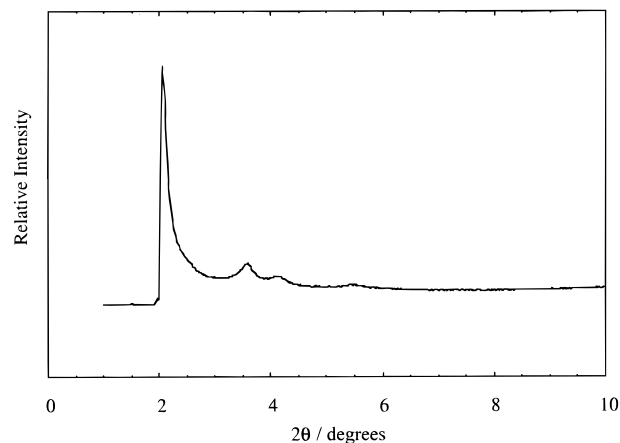
brown or black color. Calcination times were increased to 5–6 h at the maximum temperature of 973 K, but this most severe treatment still only resulted in materials that were of a “salt-and-pepper” coloration. Apparently, part of the surfactant (and/or acetylacetonate ligand) had been retained in the material even after severe oxidation treatments.

Since calcination was apparently not capable of completely removing impurities from the mesoporous titania materials, an alternative extraction method was tested. This method was developed recently by Antonelli and Ying for the synthesis of mesoporous niobia.<sup>23</sup> Nitric acid was used to cleave the bond between the anions and the transition metal atoms. The procedure appeared to have worked with mesoporous niobia but had not yet been demonstrated with mesoporous titania. The surface area of a representative sample subjected to the extraction procedure is included in Table 1. In general, high surface area materials were obtained by this treatment method.

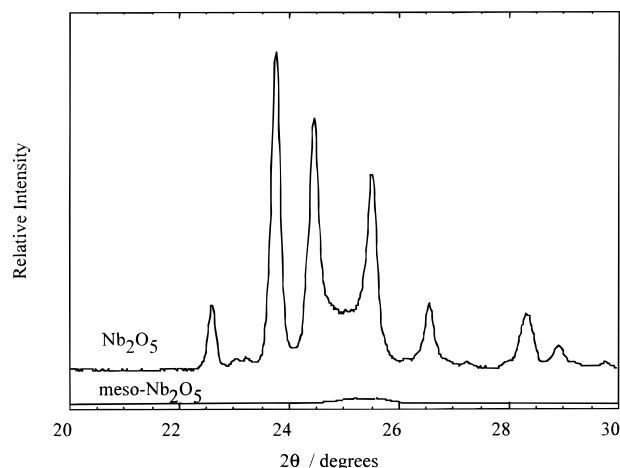
Some samples were analyzed for phosphorus, carbon, and titanium (Galbraith Laboratories, Knoxville, TN) since phosphate surfactant was used in the synthesis of mesoporous titania. The P/Ti atomic ratios for mesoporous titania calcined at 873 K and a sample extracted three times with an 8% acid solution were 0.68 and 0.57, respectively. Apparently, the acid extraction was not effective at removing phosphorus. In fact, the C/P atomic ratio in the extracted sample was very similar to that of the original phosphate surfactant. The calcination treatment, however, was sufficient to remove most of the carbon in the sample, presumably through oxidative gasification.

Figure 4 compares the crystallinity of mesoporous titania, *ns*-titania, and Degussa P25. The large and small peaks in P25 correspond to anatase and rutile, respectively. Prolonged calcination of *ns*-titania accomplished partial crystallization to mostly anatase. The phosphorus that remained in the mesoporous sample, even after calcination, likely prevented crystal growth.

A low-angle diffraction pattern of mesoporous niobia after extraction of the template is shown in Figure 5. Similar to the titania case, the large peak at low angle and the higher order reflections suggest that the pores are well-ordered. The amorphous nature of the material was confirmed by comparing the X-ray patterns of the mesoporous sample to that of niobium pentoxide, as



**Figure 5.** Low-angle X-ray diffraction pattern of mesoporous niobia after solvent extraction.



**Figure 6.** Comparison of X-ray patterns for crystalline niobium pentoxide (Aldrich) and mesoporous niobia.

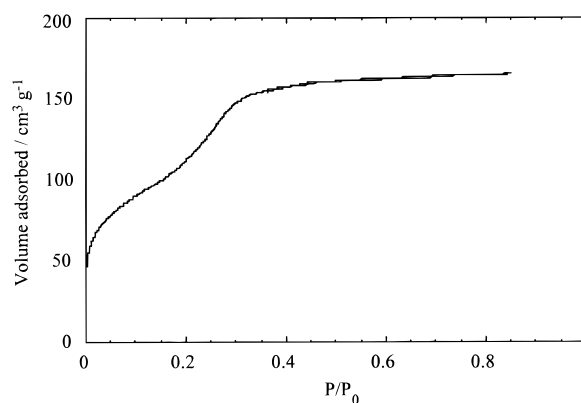


**Figure 7.** Dinitrogen adsorption/desorption isotherms of mesoporous niobia after extraction and evacuation at 453 K.

shown in Figure 6. The dinitrogen adsorption/desorption isotherms for mesoporous niobia are given in Figure 7. The surface area of 415 m<sup>2</sup> g<sup>-1</sup> is in good agreement with the range of 400–600 m<sup>2</sup> g<sup>-1</sup> reported by Antonelli and Ying.<sup>23</sup> Characterization results for the niobia samples are summarized in Table 2.

The UV reflectance spectra of the mesoporous transition metal oxides are compared to the standard materials in Figure 8. In both cases, the absorption thresholds of our samples appeared to be fairly similar to those of the reference materials, except the features were broader.

**Table 2. Characterization and Reactivity Results for Niobia Samples**

sample	surface area (m <sup>2</sup> g <sup>-1</sup> )	band gap (eV)	quantum yield <sup>a</sup>
meso-Nb <sub>2</sub> O <sub>5</sub>	415	3.29	0.0041
Nb <sub>2</sub> O <sub>5</sub>	13	3.08	0.217

<sup>a</sup> Quantum yield is defined as the molecules of acetone formed per incident photon.

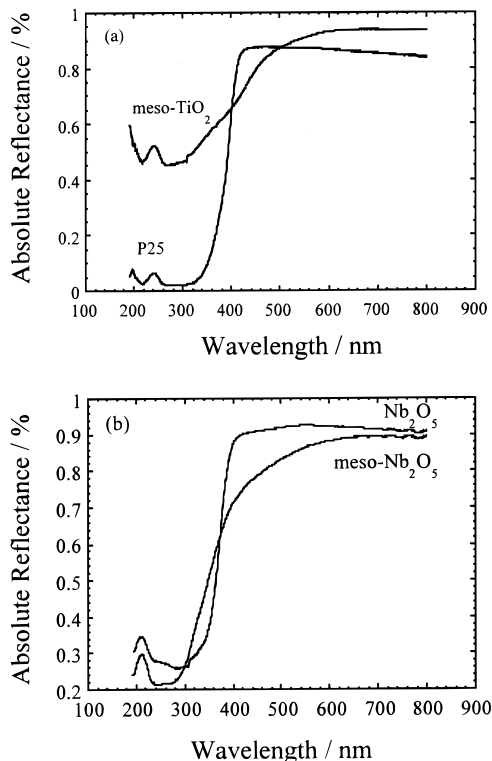


**Figure 8.** UV diffuse reflectance spectra of (a) as-synthesized meso-TiO<sub>2</sub> and Degussa P25 and (b) extracted meso-Nb<sub>2</sub>O<sub>5</sub> and Aldrich Nb<sub>2</sub>O<sub>5</sub>.

The direct optical band gap was calculated to be 3.2 eV for both meso-TiO<sub>2</sub> and Degussa P25. The calculated band gap for meso-Nb<sub>2</sub>O<sub>5</sub> (3.3 eV) was greater than that for the crystalline Nb<sub>2</sub>O<sub>5</sub> (3.1 eV), possibly due to a small quantum size effect. The band gaps reported in Table 1 show that quantum size effects were not significant in the titania materials in this study.

To test the photocatalytic activity of the materials, the well-known oxidative dehydrogenation of 2-propanol to acetone was used as a probe reaction. Acetone and 2-propanol were the major species detected. The control reactions, shown in Figure 9, demonstrate that both the catalyst and illumination were necessary to achieve reaction. A statistical analysis of the control reactions confirmed the absence of activity over a 24-h period.

A typical photocatalytic reaction over Degussa P25 catalyst is also illustrated in Figure 9. The quantum yield, defined as the number of acetone molecules formed per incident photon, was calculated to be 0.45 during the first hour of reaction. We also tested a sample of anatase (Aldrich) and measured a quantum yield of 0.41. Therefore, a relatively high quantum yield for the 2-propanol reaction is intrinsic to crystalline titania. Results from photocatalysis on synthetic titania samples are shown in Figures 10 and 11 and summarized in Table 1. Under identical reaction conditions,

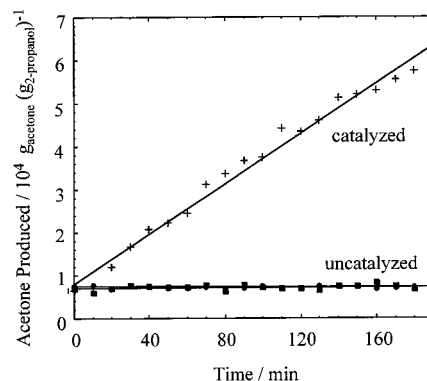


**Figure 9.** Photocatalytic production of acetone from 2-propanol over irradiated Degussa P25 titania (+). Results from runs without UV light (●) and without catalyst (■) are shown for comparison.

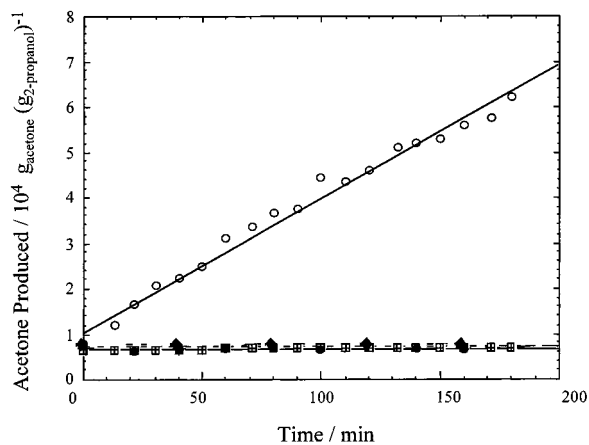


**Figure 10.** Photocatalytic production of acetone from 2-propanol over P25 (○), as-synthesized meso-TiO<sub>2</sub> (□), and as-synthesized *ns*-TiO<sub>2</sub> (●). Diamonds (◆) correspond to the control reaction without UV light.

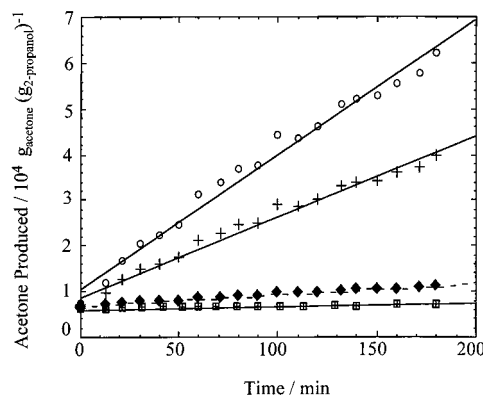


**Figure 11.** Photocatalytic production of acetone from 2-propanol over meso-TiO<sub>2</sub> calcined at 873 K for 1 h (□), *ns*-TiO<sub>2</sub> calcined at 873 K for 3 h (◆), *ns*-TiO<sub>2</sub> calcined at 873 K for 12 h (+), and P25 (○).

the quantum yields of the mesoporous samples were several orders of magnitude lower than that of P25. Poorly crystallized synthetic titania samples, prepared without surfactant, were also poor photocatalysts. Calcination of these samples for longer times (*ns*-TiO<sub>2</sub> series in Table 1) both crystallized the particles and increased their quantum yields. The approximate percentages of anatase and rutile in the sample calcined for 12 h are 80% and 20%, respectively, similar to that of P25.

Indeed, the quantum yield of this sample was 0.27, about half that of P25. Figure 11 shows the increased photocatalytic activity of these partially crystallized samples.

As a comparison, two forms of niobia were also examined for photoactivity. Similar to the titania case, the quantum yield was orders of magnitude greater over the dense, crystalline compound compared to the mesoporous, amorphous sample. These results are summarized in Table 2.

### Discussion

The characterization results confirm that a high surface area, mesoporous, Ti-containing material was synthesized by a ligand-assisted templating method. However, elemental analysis revealed that calcination and extraction did not remove phosphorus from the sample. Therefore, these titanium materials were really composites that have the surfactant (or remnants of the surfactant) attached strongly to their surfaces. This observation has also been reported by Putnam et al., who investigated similar samples.<sup>31</sup> In that study, crystalline titanium phosphates were detected by X-ray diffraction after calcination at 773 K for 24 h.<sup>31</sup> The extremely high surface area of our samples obtained after low-temperature calcination is likely due to the formation of an open mesoporous structure and the retention of a substantial fraction of the surfactant in the material. The fact that phosphorus was held tenaciously by the mesoporous titania will likely limit its possible use as a catalyst or catalyst support. Fortunately, mesoporous niobia can be synthesized with an amine template that can be removed by a solvent extraction. Elemental analysis of mesoporous niobia indicated a 6-fold reduction in surfactant loading after three extraction treatments. The high surface area of our niobia sample is attributed to the open mesoporous structure of the extracted solid.

The as-synthesized mesoporous samples were locally amorphous since no peaks were observed in the X-ray pattern at high  $2\theta$  (see Figure 6). We found it quite striking that the UV reflectance spectra of the as-synthesized materials were similar to those of bulk phase standards. However, one difference is clear: the UV absorption threshold was sharper in both crystalline standards compared to those of the mesoporous samples. A variety of microenvironments within the mesoporous samples may account for the broad features. Nevertheless, the UV reflectance spectra indicated that the mesoporous materials may function as photocatalysts since they absorbed photons of the appropriate energy range.

We chose to use the oxidative dehydrogenation of 2-propanol to acetone as a simple probe reaction for photocatalytic activity since it has a relatively high quantum yield and is simple to perform. Our measured quantum yield of 0.45 for the reaction over P25 titania is comparable to previously reported values of 0.48 by Lee<sup>30</sup> and 0.28 by Hussein and Rudham.<sup>32</sup>

The various forms of mesoporous titania, listed in Table 1, were very poor photocatalysts. Indeed, the

quantum yields for the 2-propanol reaction were orders of magnitude lower than those of P25 and anatase (Aldrich). Interestingly, poor quantum yields were observed for some of our titania catalysts that were synthesized in the absence of a template. After progressive crystallization of these nonsurfactant (*ns*) samples by prolonged calcination at high temperature, the quantum yield of the 2-propanol reaction increased by more than an order of magnitude (see Table 1). Since the surface area of these samples did not change significantly with calcination temperature, and since the band gap of the as-synthesized *ns*-titania was similar to that of crystalline titania, we suspect that the degree of crystallinity played a major role in the photocatalytic activity of titania.

Previous researchers have observed that amorphous titania materials are inactive photocatalysts. Davidson et al. showed that polycrystalline samples of titania had high photoproduction rates of dihydrogen as compared with amorphous forms.<sup>33</sup> Tanaka et al. also found that amorphous titania also gave the lowest photodegradation rate of trichloroethane and chloroacetic acid.<sup>34</sup> As mentioned earlier, Ohtani et al. determined that, for constant particle size, the photocatalytic activity of titania increased linearly with the fractional crystallinity of anatase.<sup>21</sup> Our results with nonsurfactant titania are completely consistent with the results of Ohtani et al. Apparently, crystallinity and photoactivity are inextricably linked.

The presence of defects in the amorphous samples is speculated to be the cause for the low quantum yields. These defects can act as recombination centers for the photogenerated electron-hole pair. As discussed by Ohtani et al., the defects can be present in both the bulk and the surface of the material.<sup>21</sup> It was our intention to synthesize the mesoporous transition metal oxides to obtain materials with extremely high surface areas, negligible concentrations of bulk defect centers, and optical band gaps comparable to those of bulk crystals.

Alternatively, Tanaka et al. suggest that peroxide, formed by the reaction of dioxygen with a surface hydroxyl, impairs the photocatalytic action of titania.<sup>34</sup> Samples with high concentrations of surface hydroxyls (i.e., amorphous titanias) will therefore be less effective photocatalysts. However, hydroxyl radicals are important intermediates in the photooxidation of organics over irradiated titania.<sup>35</sup> Thus, we believe that a high defect density is the major reason that amorphous materials are inefficient photocatalysts.

The relative inactivity of our mesoporous titania samples can be attributed to a high surface concentration of defects which can act as surface electron-hole recombination sites and/or the poisoning of catalytic surface sites by the phosphorus remaining from the surfactant. For the titania samples, these two effects may be interrelated and cannot be separated at this time. However, our mesoporous niobia material also showed very poor photoactivity compared to a crystalline sample. Since most of the surfactant was removed

(33) Davidson, R. S.; Morrison, C. L.; Abraham, J. *J. Photochem.* **1984**, *24*, 27.

(34) Tanaka, K.; Capule, M. F. V.; Hisanaga, T. *Chem. Phys. Lett.* **1991**, *187*, 73.

(35) Turchi, C. S.; Ollis, D. F. *J. Catal.* **1990**, *122*, 178.

(32) Hussein, F. H.; Rudham, R. *J. Chem. Soc., Faraday Trans. 1* **1984**, *80*, 2817.

from the mesoporous sample, the low activity is attributed to the detrimental effect of surface defects on photocatalysis over amorphous materials. We propose that, in addition to bulk defects, surface defects play an important role as recombination centers on transition metal oxide photocatalysts. These results suggest that highly defective thin films of oxide semiconductors will need to be partially crystallized prior to use as photocatalysts.

### Conclusions

Mesoporous transition metal oxide molecular sieves having extremely high surface areas were successfully synthesized by a previously reported ligand-assisted templating method. Although the mesopore structure was well-ordered, the metal oxides were locally amorphous. In the case of mesoporous titania, phosphorus from the template was bound so strongly to the molecular sieve that it could not be removed by either calcination or solvent extraction. In contrast, solvent

extraction was effective at removing the amine template from mesoporous niobia. The quantum yield for the photocatalytic reaction of 2-propanol to acetone was orders of magnitude lower on the molecular sieves compared to the appropriate crystalline materials, even though the optical band gaps were similar. Results from control experiments on partially crystallized titania samples indicate that surface defects on the transition metal oxide molecular sieves may catalyze the recombination of photogenerated electron-hole pairs and lower photocatalytic activity.

**Acknowledgment.** We gratefully acknowledge the National Science Foundation (SGER 9617250 and GER 9452654) and the Virginia Academic Enhancement Program for support of this work. R.J.D. acknowledges partial support from a National Science Foundation Young Investigator Award (CTS-9257306).

CM980050R